Evaluation of L5 Band GNSS for Use in Time-Transfer

Ben Pera, Andrew Novick, *National Institute of Standard and Technology*

BIOGRAPHY

Ben Pera Ben Pera is an engineer in the Time Realization and Distribution Group at the National Institute of Standards and Technology (NIST). His work is centered around system and hardware design for traceable time transfer. These activities include GNSS time transfer, TWSTFT, and local time and frequency distribution and measurement.

Andrew Novick Andrew Novick is an electrical engineer in the Time Realization and Distribution Group in the Time and Frequency Division at NIST. He manages and maintains the remote clock and oscillator calibration services and other monitoring and research projects. Novick created and maintains the national web clock, www.time.gov, and he is the division's Quality Manager.

ABSTRACT

The L5 frequency band of GPS features a higher power, higher code rate, and superior performance in GNSS denied or degraded environments. GPS L5 is pre-operational at time of writing with 17 satellites but has sufficient coverage for testing and utilizing its performance almost fully. In this paper, the satellite metadata, signal to noise, position uncertainty, and time uncertainty are tested under various conditions. The inclusion of the L5 frequency band shows slightly improved performance under normal rooftop antenna conditions and significantly improved performance in degraded signal environments. Incorporating L5 band signals into GNSS time transfer provides opportunities to use traceable time transfer in previously inaccessible situations and to improve uncertainty in current applications.

I. INTRODUCTION AND BACKGROUND

GNSS signals exist across the L-band (1 GHz to 2 GHz), and signals have been added recently as part of modernization efforts or new constellations. In time transfer, the most commonly used signals are the GPS L1 and L2 bands. The use of both frequencies in conjunction allows ionospheric delay measurements, greatly enhancing accuracy. A third civilian signal is being added to GPS, L5, designed for better accuracy and interference resistance (including multi-path).

Three other constellations can be used with dual-frequency capability: Galileo, GLONASS, and BeiDou. Galileo has a similar set of signals, E1, E5a, E5b, and E6. E1 and E5a overlap with L1 and L5 signals, making them directly comparable to GPS.

1. Signal Characteristics

Each signal features a different carrier frequency and has a different modulation scheme, code rate, and nominal power level. Table 1 summarizes the signals that are be analyzed in this paper. We note the higher code rate and higher power level of the L5 and E5a bands compared to L1/L2 and E1.Signal specifications are posted in the GPS and Galileo interface control documents (GPS (2022) and GAL (2023)). The GLONASS signals also occupy three distinct bands, with a fundamental difference being that they are frequency division multiple access (FDMA) signals rather than code division multiple access (CDMA). Each GLONASS satellite is identified by a different frequency offset, rather than data embedded on the code.

2. Current and Future Coverage of L5 Band GNSS

Both GPS and Galileo operate constellations with 24 active satellites required, keeping spare satellites in each orbital plane for redundancy. As of December, 2024, Galileo is fully online, supporting all three previously listed signals. The GPS constellation, currently fully supports L1 and L2, and has 17 operational L5 satellites, with an additional L5 satellite in on-orbit testing. For this reason, L5 GPS only covers part of the globe at a time with the minimum required four satellites in view. Until 24 L5 satellites are online, the L5 signal broadcasts its status as "unhealthy" causing most receivers to reject the signal and to not use it in their solutions. The three remaining satellites in GPS Block III are declared ready for launch , with all three expected to be launched by 2026. With the announced tentative future launch dates for the remaining satellites, GPS L5 should be declared operational in mid 2028. Projected launch schedules are mentioned in the Air Force budget estimates, USA (2024).

https://doi.org/10.33012/2025.19944

GNSS Signal	Center Frequency	Modulation Scheme	Code Rate	Minimal Received Power[1]
L1C	1575.42 MHz	TMBOC	1.023 MHz	-158.5 dBW
L2C	1227.60 MHz	BPSK	1.023 MHz	-161.5 dBW
L5	1176.45 MHz	QPSK	10.23 MHz	-157.9 dBW
E1	1575.42 MHz	CBOC	1.023 MHz	-157 dBW
E6	1278.75 MHz	BPSK	5.115 MHz	-155 dBW
E5a	1176.45 MHz	altBOC	10.23 MHz	-155 dBW

Table 1: Characteristics of GPS and Galileo signal bands; this is a simplification that outlines key performance differences and should not be used for hardware design.

3. Challenges of L1/L2 Band GNSS for Time Transfer

There are a number of issues that limit the performance of dual-band GNSS for time transfer, even in fixed locations with well-placed antennas. Some of these are inherent to all microwave-band one-way or common-view time transfer, such as ionospheric and tropospheric delays, and some are unique to GNSS or constellation-based time transfer, such as multi-path interference and jamming. There are many more performance limitations to GNSS which will not be discussed here.

Ionospheric and tropospheric delays are the result of varying electron content in the upper atmosphere due to ionizing radiation and changing permittivity in the lower atmosphere due to moisture content (Hoque and Jakowski (2012)). This causes variable time delays that need to be compensated for if high quality position or time is desired. Modern dual-frequency receivers already largely solve this problem in real-time, measuring differential delays between bands for ionosphere-free delay estimates, and using stored seasonal and geographical models of tropospheric conditions. Unfortunately, the effects are not totally cancelled and residual errors remain that can be made smaller with measurements of more bands and satellites or nearly removed using post processing methods utilizing globally dispersed monitoring stations (e.g. precise point positioning, PPP).

Multi-path interference (MI) occurs when a signal can take multiple paths to its destination, causing interference when the signal is received. In the case of GNSS, this is most often due to reflection off of buildings or other structures as well as the ground when the observed satellite is at a low elevation. MI can cause a receiver to see a signal later than otherwise, causing a problematic satellite range value, or if detected by the receiver as MI, one fewer satellite observation. Detecting and preventing MI reception can be accomplished with good antenna placement, ideally as the highest structure in the area. Antenna designs to prevent reception of counter-polarized waves created by reflection and with structures to prevent below-horizon pickup also aid in MI resistance. Higher code rates and bandwidth, such as are present on L5, help mitigate MI by giving the receiver a finer time accuracy to detect delays and more range to detect reflected vs direct signal strength as described in Tsang et al. (2023). As uses for GNSS time transfer are increasing in urban canyon environments, preventing MI becomes a bigger concern.

II. SIMULATION

To understand the impact of the partial L5 constellation, we simulated the ground coverage with a varying minimum number of satellites visible. For time transfer, since location is almost always fixed, having fewer than four satellites does not always result in the loss of time transfer capabilities. Even so, on average, 75% of the globe has four or more L5 satellites in view. If this threshold is brought to three or more satellites, 90% of the globe is covered. This coverage is skewed towards the poles by the nature of the constellations design, compensating for the lower observed elevation of the satellites at more extreme latitudes.

The orbital parameters of satellites in the GPS constellation are outlined by the GPS ICD (GPS (2022)) and the status of each satellite is updated and posted by the US Coast Guard at Center (2025). Using these parameters, the coverage of the constellation can be simulated. To do this, for each time of the sidereal day (approximate repeat period found in Agnew and Larson (2006)), the position of each satellite in the constellation is simulated. This is done using MATLAB's satellite simulation toolbox, which handles orbital propagation and coordinate reference frame conversion. Next, the number of satellites visible at a location of interest is determined by checking if it is obscured by the Earth. For this analysis, a spherical model of the earth is used due to the simplicity of angle calculations. This method slightly overestimates coverage by not accounting for obstructions at low angles. The process of counting lines of sight to satellites is repeated for all simulated locations, in this case, an approximately even spread of 15,000 points across the globe generated using a fibonacci spiral. An instantaneous coverage map is created at simulated time intervals of approximately 90 seconds (1/1000 of a sidereal day). For more easily viewable data, these maps are combined by computing the fraction of time each geographic point has four or more visible satellites. This results in a map of how much GPS coverage is expected at any location on Earth.

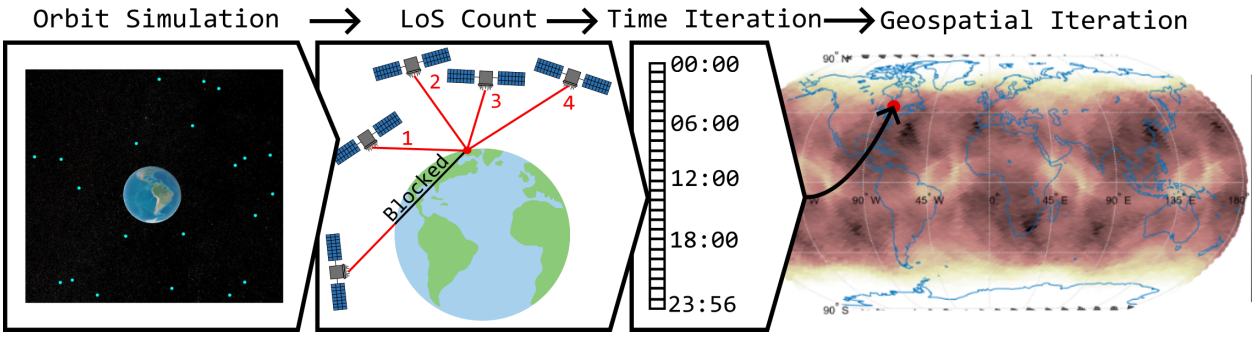

FIGURE 1: Simulation procedure to produce coverage maps

When calculated using current satellites broadcasting L1 and L2 frequencies, as expected, there is nowhere on Earth that has fewer than four satellites in view at any time, the minimum required for typical usage. When the list of satellites is modified to only include those broadcasting L5 signals, the maps show geographically distributed areas of varying coverage levels. On average, 75% of Earth is receiving L5 signals from four or more satellites. This coverage is concentrated at the poles, with middle latitudes having the most breaks in coverage. Even so, all points receive L5 coverage at least 58% of the time. For fixed position timing applications, fewer satellites are required to be in view. With a threshold of one satellite, everywhere on Earth could lock on in this manner, and with a threshold of two, most locations have continuous coverage, and some areas have up to 10% breaks in coverage.

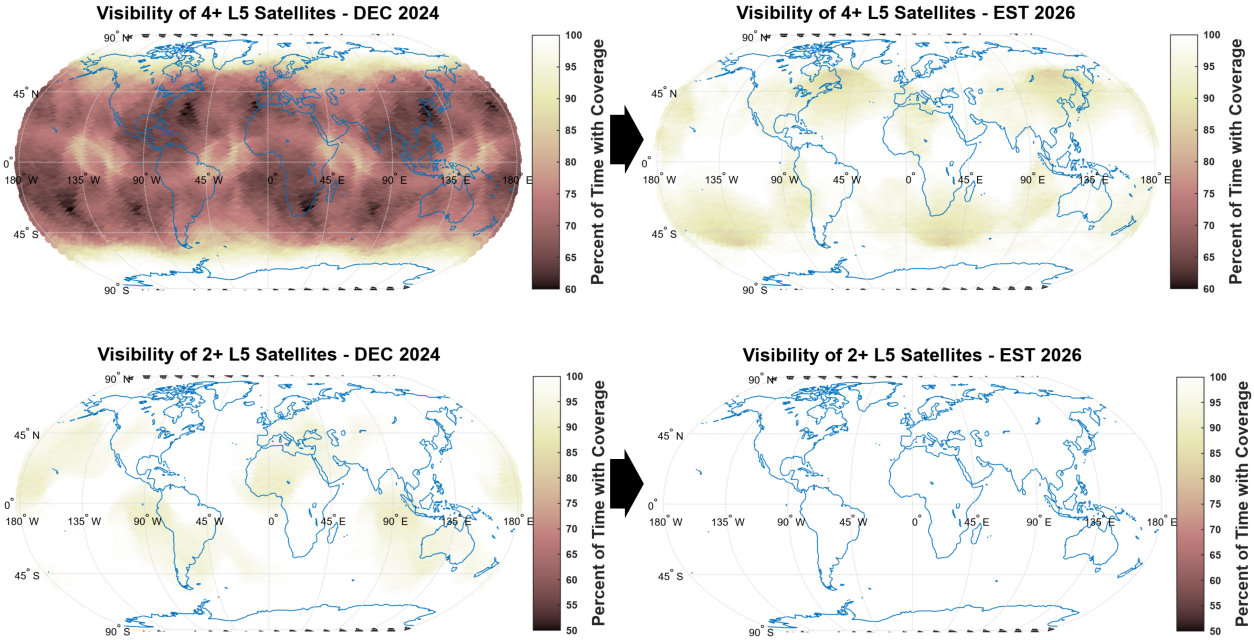

FIGURE 2: Simulated coverage patterns of GPS L5

Although the L5 signal will not be designated as healthy until a full 24 satellite constellation is completed (likely by 2028), significantly improved coverage can be had with the partial, 21 satellite constellation expected in 2026. When these satellites are added to the constellation of the previous simulation, average global coverage is increased to 97.5%, and minimum coverage is increased to 85% (assuming placement in appropriate orbits). When the threshold is reduced to three or more satellites in view, minimum coverage is over 98%. This aligns with specifications provided for the GPS network operating with a reduced number of satellites.

III. STATIC RECEIVER TESTING

To test the performance of L5 band signals in an obstructed environment, signal degradation was compared to that of of other GNSS bands. This provides a sense for how much more obstruction or interference L5 can withstand.

1. Test Environment Setup

The measurement of degradation D presented here is the decrease in receiver-reported carrier-to-noise density C/N_0 from a reference location to a location under test.

$$D = C/N_{0-\text{Ref}} - C/N_{0-\text{Test}} \tag{1}$$

Because C/N_0 is largely a product of the antenna/cable/receiver combination, the same model of receiver, cable length, and tri-band surveying antenna were used for both the reference and test devices.They were both run concurrently on the rooftop for a short period to verify that they performed similarly. A month's long data run was collected between October 2024 and December 2024 with the test antenna placed indoors in a lab on the top floor of NIST in Boulder, Colorado and the reference antenna placed on the rooftop above the lab. Both receivers were fed with the same 10 MHz signal and PPS signal, both directly derived from UTC(NIST).

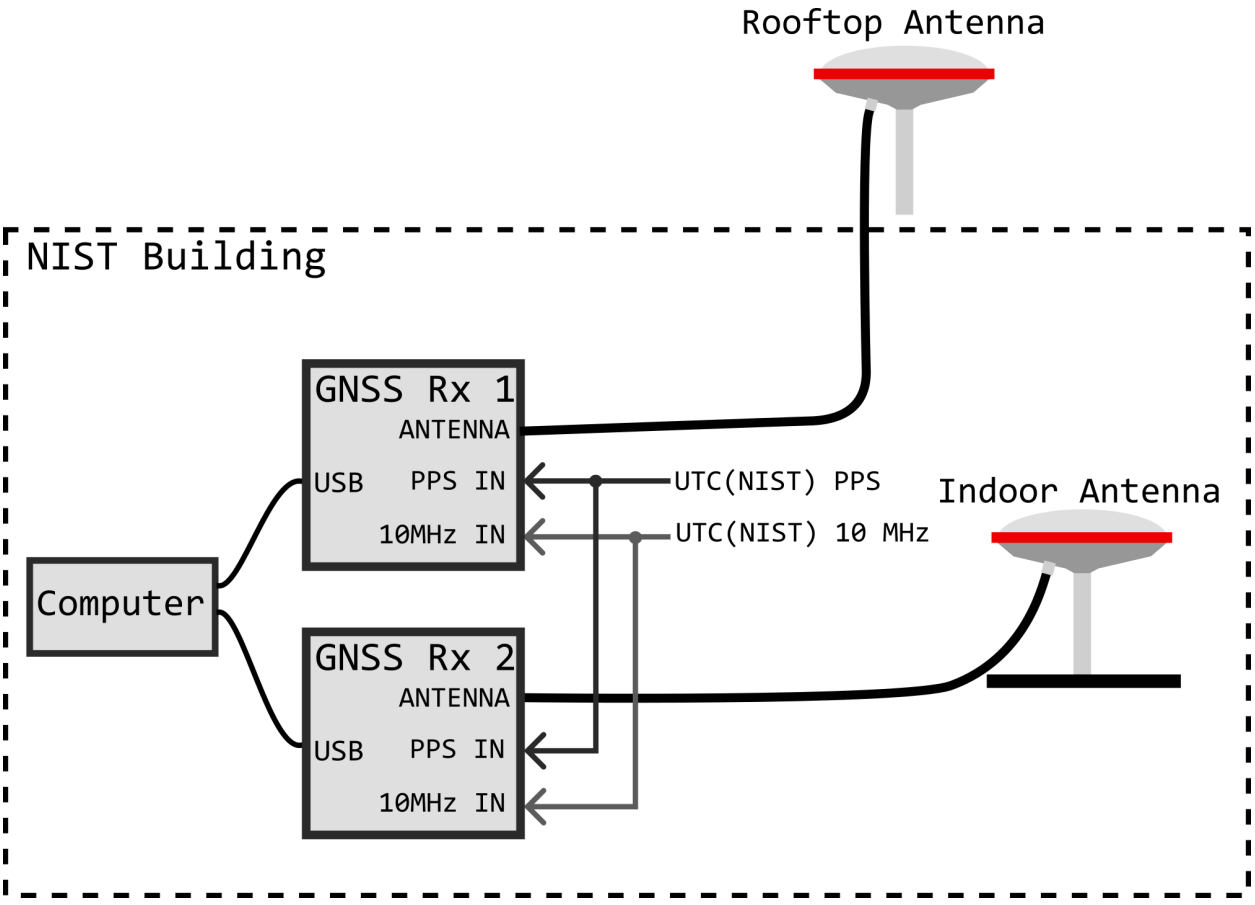

FIGURE 3: Testing configuration for the static receivers

2. Data Analysis

All data were recorded in the SBF data format and processed using a combination of receiver manufacturer provided tools for file conversion and custom python scripting for analysis. Of immediate interest is the measurement of the C/N_0 at the test locations and in different signal bands. Average degradation is calculated with each sample weighted evenly. Table 2 summarizes the relevant C/N_0 data, as well as the measured degradation for each signal. Of note is that the receiver was unable to lock on to the L1 P-code indoors, which indicates that the C/N_0 was below the receiver's stated threshold of 10 dB-Hz, and degradation for that signal above 28 dB on average.

GNSS Signal	C/N_0 with Clear Sky	C/N_0 Indoors	Degradation
L1C/A	44.0 dB-Hz	36.9 dB-Hz	7.1 dB
L1PY	38.1 dB-Hz	$\leq$ 10 dB-Hz	$\geq$ 28 dB
L2C/A	42.4 dB-Hz	33.5 dB-Hz	8.9 dB
L2PY	38.1 dB-Hz	22.8 dB-Hz	15.3 dB
L5	45.0 dB-Hz	34.8 dB-Hz	10.2 dB
E1	42.9 dB-Hz	38.3 dB-Hz	4.6 dB
E6	45.4 dB-Hz	35.2 dB-Hz	10.2 dB
E5a	42.9 dB-Hz	35.7 dB-Hz	7.2 dB
E5b	45.4 dB-Hz	35.9 dB-Hz	9.5 dB

Table 2: C/N_0 of GNSS Signals in Obstructed Environments

Within the GPS signals, the L1 C/A and L2 C/A have the lowest signal degradation to the indoor environment. This may be surprising considering the stated goals of L5 performing better. While it is true that lower precision codes on L1 and L2 can penetrate through building materials well, their high precision components do not. This, along with the fact that L5 has higher transmitted power than L1 and L2, means the high precision L5 signal can serve to greatly improve accuracy in indoor and urban environments.

For further analysis, to ensure that changes in C/N_0 due to external factors that vary spatially or in time are not misapplied to each signal, degradation is calculated for each satellite at each measurement times. This method allows for the determination of covariance of degradation with satellite elevation and location in the sky. Analyzing degradation compared to elevation is somewhat hindered by the fact that each MI and obstructed environment will be unique, particularly when looking at the finer structure. Despite this, the signals can still be compared for their relative behavior. The exact value of degradation changes from the ones shown in table 2, due to averaging at each spatial coordinate. As should be expected, signal degradation is larger at lower elevations, as the signal must pass through more material and MI due to vertical walls interferes more. At elevations below 10 degrees, there is an apparent decrease in degradation, which is due to the interference at the rooftop receiver from geographic obstructions such as the nearby mountains and buildings. This decreased reference C/N_0 causes the apparent degradation to decrease.

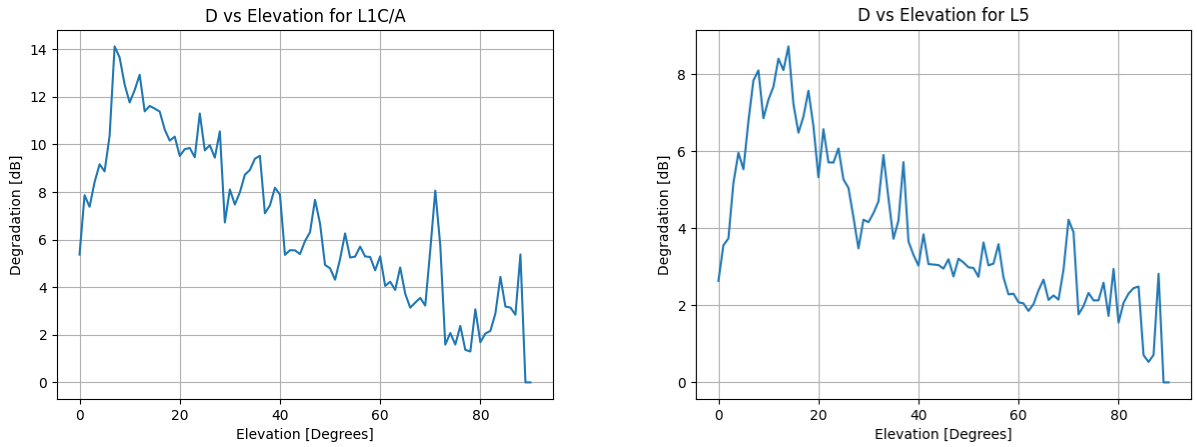

FIGURE 4: Comparison of degradation vs elevation for GPS signals

Plotting the averaged D at each point in the sky provides deeper insight into how the signals respond to obstructions. Not the entire sky is covered by passing satellites, even during a full cycle of the GPS constellation. Due to the 55° orbital inclination and our latitude of observation of 40° N, there is a ”hole” of missing observations in the northern part of the sky beyond 15°

from vertical. There is also a persistent structure in the outermost 10° in the southwest, where the mountains obstruct all direct observations, leading to misleading D measurements.

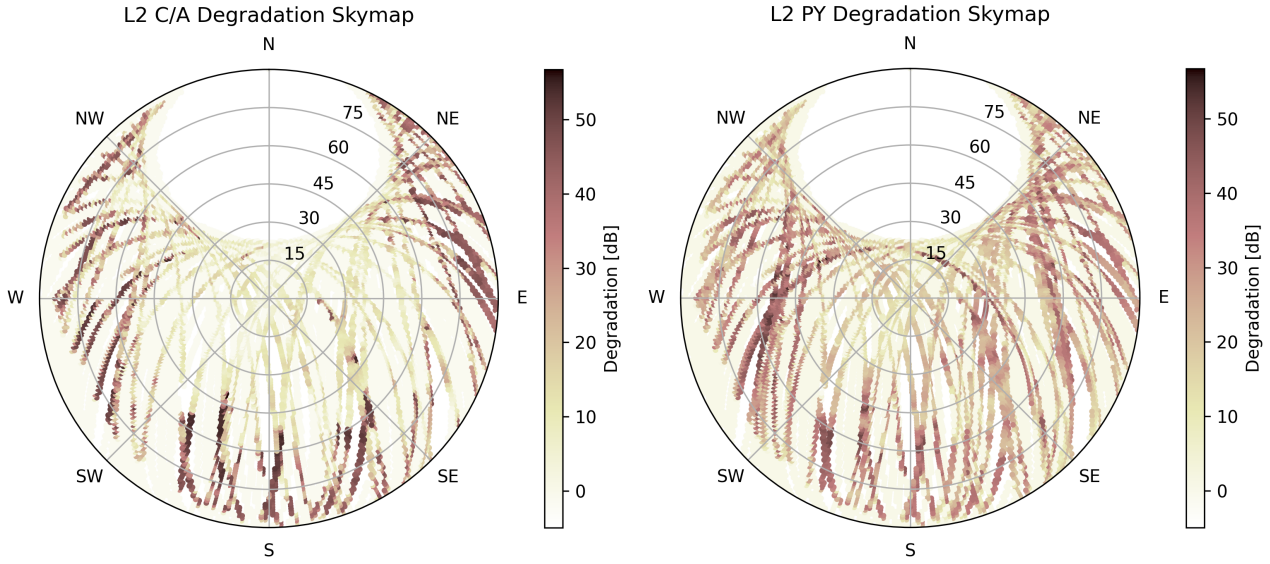

FIGURE 5: Comparison of L2 degradation across the sky

L2 C/A has much better signal penetration in general than the accompanying P(Y) code. However, the C/A code sees markedly stronger degradation biased in particular directions within 30^o of the horizon. This can be explained by the presence of more building, as the structure is narrow and aligned NE/SW.

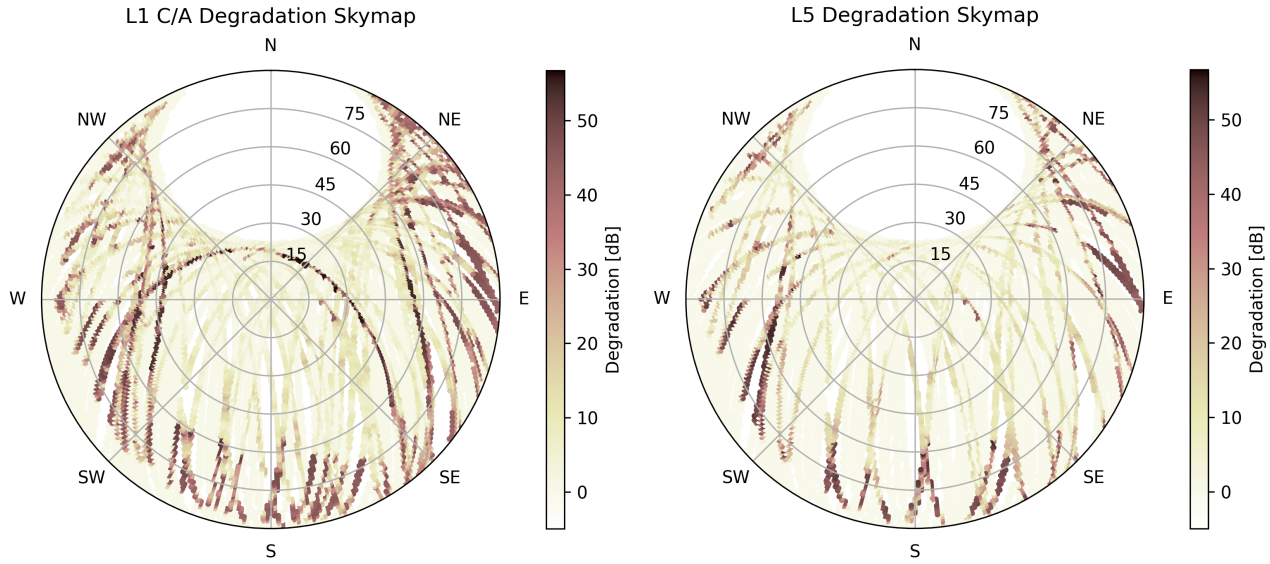

FIGURE 6: Comparison of L1 C/A and L5 degradation across the sky

From figure 6, we find that L5 signals have better penetration through the building than all of the others. There is still strong degradation at very low angles, but even then, significant signal still passes through. This improved penetration should lead to

much better performance in indoor or urban canyon environment, potentially making portable time transfer receivers possible that do not need to have cables routed outside for performance to be acceptable.

IV. RECEIVER IN TRANSIT

Most current terrestrial needs for time transfer are physically static in nature: national laboratories, stock exchanges, cellular base stations, etc. However, there are uses for precision aligned time in non-stationary situations: mobile RF test instrumentation, vehicle mounted radar, ultra-high-speed communications. As these technologies advance, they require ever tighter timing tolerances.

1. Test Environment

To test accuracy of GNSS while in-transit with L5 enabled, the same antenna and receiver was mounted to a car and put under test. The test equipment consisted of an cesium beam clock that was monitored for drift before and after the experiment against UTC(NIST) as well as a time interval counter (TIC) to monitor the difference between the clock and the receiver's PPS output. The whole assembly mounted in the car was then driven through city streets and on a highway to and and back from NIST's radio station, approximately a 90 minute drive away. Figure 7 shows how the system was connected. The GNSS receiver was connected to the 10 MHz from the cesium clock. In order to verify that the resultant measurement is not a measurement of the receiver's ability to lock on to an external frequency, we later ran a test in the laboratory measuring the time output noise with and without a 10 MHz frequency reference attached to the receiver's connector. In figure 8, it is shown that while the character of the noise is different, it is of very similar magnitude.

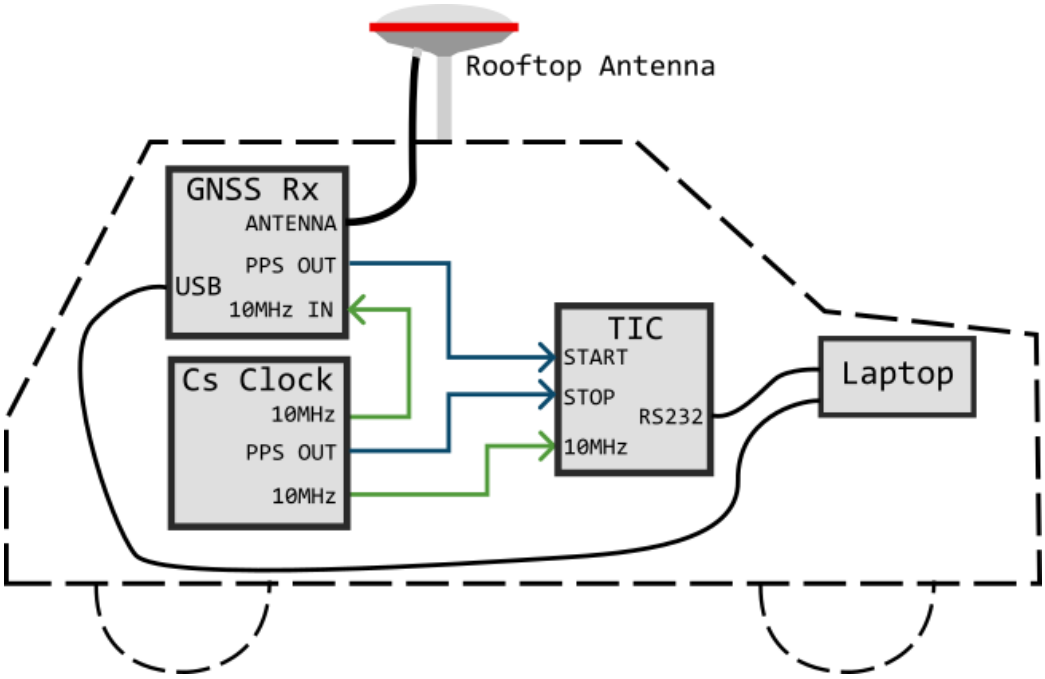

FIGURE 7: Testing configuration for the receiver in transit

2. Analysis

The output of the receiver contains a semi-periodic and known error due to drifting of its internal clock and limited output step resolution. This error changes over time, increasing until it has reached the step resolution where the receiver can then adjust its output to correct for the change. Commonly this is known as 'sawtooth error', and the receiver outputs this value, allowing for it to be removed digitally after measurement. The peak to peak sawtooth fluctuations vary by receiver, and in this case, are of 25 ns in magnitude. When this is subtracted from raw TIC measurements, as shown in figure 9, the observed short-term instability decreases significantly. For any real-time applications, this must be corrected in hardware or steering algorithms. In a GPS disciplined oscillator (GPSDO), this is typically done within a digital steering algorithm. If only long-term stability is needed, this sawtooth error can be removed by averaging with a long enough period for the reduced noise to fall below other

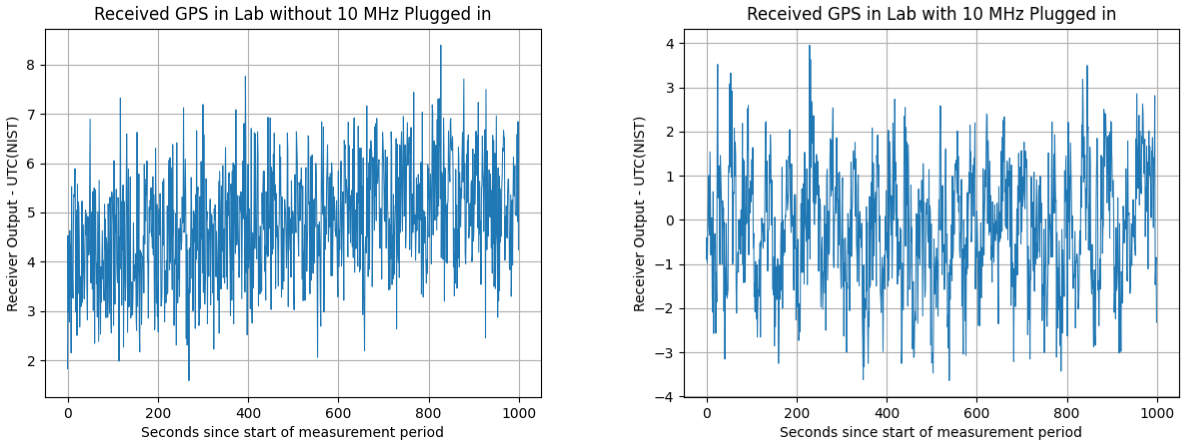

FIGURE 8: Comparison of receiver stationary noise with and without external 10 MHz connection

noise sources in the received GPS time.

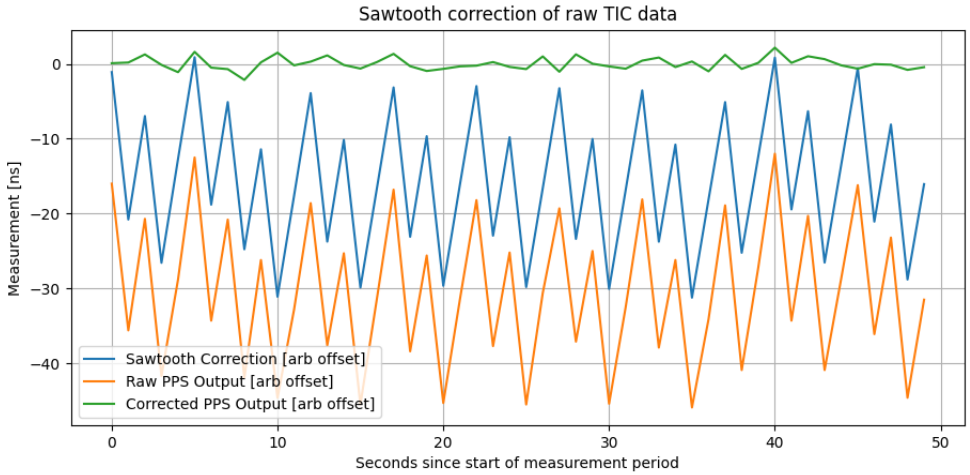

FIGURE 9: Process of subtracting sawtooth error from TIC measurements

During the trip, the GNSS receiver and the cesium beam tube never deviated by more than 50 ns. Deviations were caused by the GNSS receiver changing between different solution modes. In normal usage, the receiver takes into account real-time approximations of precise point positioning (PPP) information broadcast by a private L-band satellite. When this transmission is obstructed, the receiver uses satellite-based augmentation system (SBAS) broadcasts where available A third situation that can arise is if the SBAS satellite is obstructed as well, putting the receiver into stand alone mode, using solely the received GNSS signals. While GNSS stand alone is not particularly inaccurate, when the receiver switches to this mode, it recalculates it's solution from scratch, causing large phase steps on the order of 20 ns to 50 ns. During the 1 hour and 14 minute recorded period, the receiver switched to SBAS mode 14 times, for no more than 10 seconds each, and to stand alone mode three times, for a total of 276 seconds. The L-band interruption where SBAS was still visible were not correlated to any significant events on the road. When in SBAS aided mode, the time offset increased between four to eight nanoseconds, before returning when switching to real-time PPP mode. The interruption of both SBAS and L-band occurred while passing beneath underpasses in slow traffic. This provides further explanation for the increased noise in this period as it has significant opportunity for MI problems.

If the major interruptions are looked past, as would be reasonable for a system that could ensure visibility of geostationary

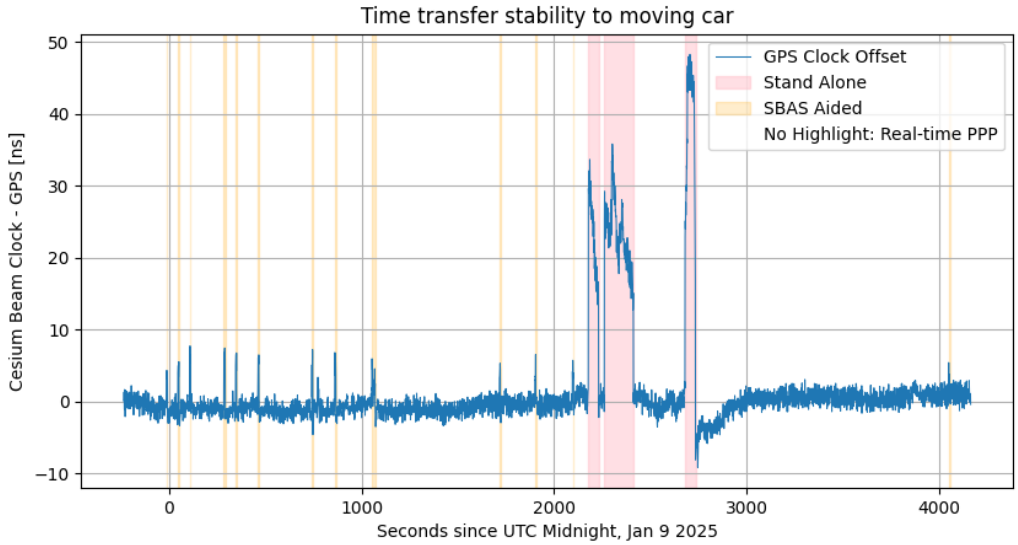

FIGURE 10: Record of clock offset during transit

satellites, such as a drone or airplane, the time deviations do not exceed 10 ns. The short term instability is on the order of 2 ns, with slow, hour scale drifts reaching up to 5 ns in the short observed period. Achieving similar performance without real-time regional corrections may be possible, but would require a receiver optimized to operate in this mode alone. Coupled with a high-quality local oscillator, a GPS disciplined oscillator with nanosecond level stability for mobile applications is fully realizable. Long term time offset drift and absolute inaccuracies may still be present on receivers using L5, and further research is needed to verify time-transfer accuracy levels.

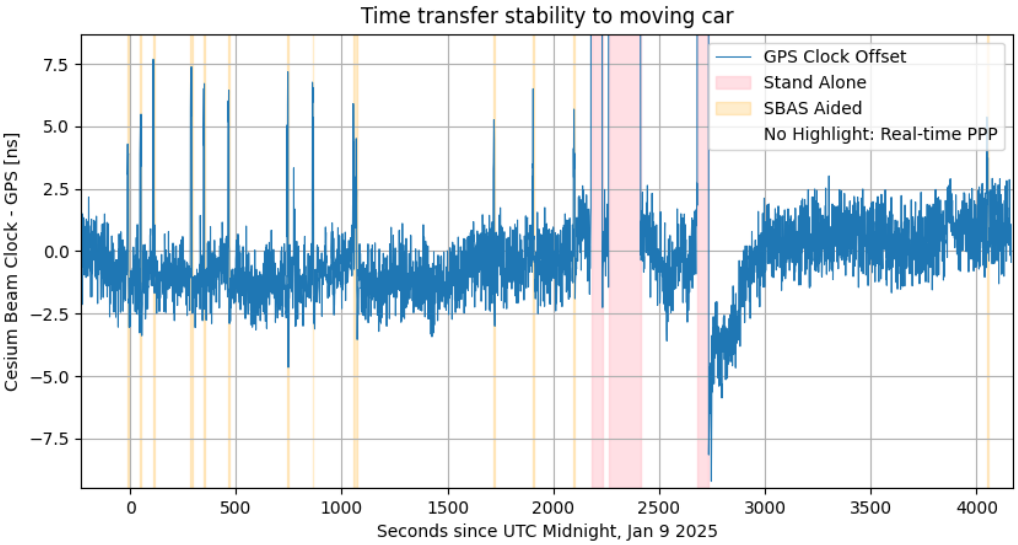

FIGURE 11: Record of clock offset during transit, zoomed to ignore loss of L-band

V. CONCLUSIONS

L5 band provides enhanced performance, showing more than 5dB lower signal degradation than comparable precision L2 P(Y) signals and more than 15 dB lower signal degradation than L1 P(Y) signals. When used in indoor or urban canyon environments, lower degradation improves position and time accuracy. This performance is currently realizable with limited interruptions, and within a few years should be at full capacity. The technology also makes possible mobile time sources with short-term stability at the few nanosecond level.

ENDORSEMENT

Certain equipment, products, or proprietary methods are identified in this paper in order to specify the experimental procedure adequately. Such identification is not intended to imply recommendation or endorsement of any product or service by NIST, nor is it intended to imply that the materials or equipment identified are necessarily the best available for the purpose.

REFERENCES

(2022). *IS-GPS-200*. US Space Systems Command. Available at `https://www.gps.gov/technical/icwg/` (2025/01/24).

(2023). *Galileo OS SIS ICD*. European Union. Available at `https://www.gsc-europa.eu/sites/default/files/sites/all/files/Galileo_OS_SIS_ICD_v2.1.pdf` (2025/01/24).

(2024). *USAF 2025 Budget Estimates Procurement, Space Force*. Unites States Air Force.

Agnew, D. C. and Larson, K. M. (2006). Finding the repeat times of the gps constellation. *GPS Solutions*, 11:71–76.

Center, U. S. C. G. N. (2025). Gps constellation status. Available at `https://navcen.uscg.gov/gps-constellation?order=field_nanu_type&sort=asc` (2025/01/17).

Hoque, M. M. and Jakowski, N. (2012). Ionospheric propagation effects on gnss signals and new correction approaches. In Jin, S., editor, *Global Navigation Satellite Systems: Signal, Theory and Applications*, pages 381–404. InTech.

Tsang, C. L., Luo, Y., Xu, B., and Hsu, L.-T. (2023). Cn0 assessment based on gps l5l1ca signal acquisition in open-sky-light-urban-dense-urban-indoor environments with extended coherent integration time. *Journal of Aeronautics, Astronautics and Aviation*, 55(2):169–183.